114. Schmidt K (1984) Invariants for finitary isomorphisms with finite expected code lengths. Invent Math 76:33–40
115. Schmidt K (1990) Algebraic ideas in ergodic theory. AMS-CBMS Reg Conf 76
116. Schmidt K (1995) Dynamical systems of algebraic origin. Birkhauser, Basel
117. Schwartz M, Bruck S (2008) Constrained codeds as networks of relations. IEEE Trans Inf Theory 54:2179–2195
118. Seneta E (1980) Non-negative matrices and Markov chains, 2nd edn. Springer, Berlin
119. Shannon C (1948) A mathematical theory of communication. Bell Syst Tech J 27:379–423,623–656
120. Sinai YG (1968) Markov partitions and C-diffeomorphisms. Funct Anal Appl 2:64–89
121. Smale S (1967) Differentiable dynamical systems. Bull Amer Math Soc 73:747–817
122. Trachtman A (2007) The road coloring problem. Israel J Math, to appear
123. Tuncel S (1981) Conditional pressure and coding. Isr J Math 39:101–112
124. Tuncel S (1983) A dimension, dimension modules and Markov chains. Proc Lond Math Soc 46:100–116
125. Wagoner J (1992) Classification of subshifts of finite type revisited. In: Walters P (ed) Symbolic dynamics and its applications. Contemp Math 135:423–444
126. Wagoner J (2004) Strong shift equivalence theory. In: Walters P (ed) Symbolic dynamics and its applications. Proc Symp Appl Math 60:121–154
127. Walters P (1982) An introduction to ergodic theory. Springer Grad Text Math 79. Springer, Berlin
128. Walters P (1992) Symbolic dynamics and its applications. In: Walter P (ed) Contemp Math 135. AMS, Providence
129. Ward T (1994) Automorphisms of Z^d-subshifts of finite type. Indag Math 5:495–504
130. Weiss B (1973) Subshifts of finite type and sofic systems. Monats Math 77:462–474
131. Williams RF (1973/74) Classification of subshifts of finite type. Ann Math 98:120–153; Erratum: Ann Math 99:380–381
132. Williams S (2004) Introduction to symbolic dynamics. In: Williams S (ed) Symbolic dynamics and its applications. Proc Symp Appl Math 60:1–12
133. Williams S (2004) Symbolic dynamics and its applications. In: Williams S (ed) Proc Symp Appl Math 60. AMS, Providence

Synchronization Phenomena on Networks

GUANRONG CHEN[1], MING ZHAO[2], TAO ZHOU[2], BING-HONG WANG[2,3]
[1] Department of Electronic Engineering, City University of Hong Kong, Hong Kong, China
[2] Department of Modern Physics and Nonlinear Science Center, University of Science and Technology of China, Hefei Anhui, China
[3] Institute of Complex Adaptive Systems, Shanghai Academy of System Science, Shanghai, China

Article Outline

Glossary

Synchronization A problem in time-keeping, requiring the coordination of events to operate a system or a task in unison.

Distance A measure between two nodes, defined as the number of edges connecting them through the shortest paths.

Average distance The mean distance, averaged over all pairs of nodes on the network.

Clustering coefficient The probability that two randomly-selected neighboring nodes of a node are directly connected each other.

Node-degree The number of edges incident from a node.

Random-graph network A type of graph obtained by starting with a set of nodes and then adding edges between them at random.

Small-world network A type of graph in which most nodes are not neighbors of each other, but most nodes can be reached from any other node by a small number of connection steps; thus, a small-world network is highly clustered like a regular graph, and yet with a small average distance, just like a random graph.

Scale-free network A type of graph in which a small number of nodes have a large number of connections while a large number of nodes have a small number of connections, whose node-degree distribution typically follows a power-law form, with both structure and dynamics being independent of the network size.

Node-betweenness A measure of the extent to which a given node is occupied by the amount of information passing through it via shortest paths between other nodes, namely, the portion of shortest paths between all pairs of nodes which have data traffic going through this particular node in the network.

Definition of the Subject

The subject under consideration is synchronization on complex networks, with respect to the phenomena and

particularly the ability of achieving synchrony of a network of dynamical systems. The subject of synchronization is quite old, but it is a significant one continuously calling for serious and systematic investigation. Ever since the careful study of two synchronous pendulum clocks by the great Dutch scientist Christian Huygens in 1665, the subject has evolved to be an independent and indispensable field of scientific research. The current study of complex networks, on the other hand, is pervading all kinds of sciences, ranging from physical to biological, even to social sciences. Its impact on modern engineering and technology is prominent and will be far-reaching. Typical complex dynamical networks include the Internet, the World Wide Web, various wireless communication networks, metabolic networks, biological neural networks, social relationship networks, financial and economic networks, and so on. As it has turned out today, the study of synchronization phenomena and synchronous behaviors of dynamical systems such as oscillators on complex networks has become overwhelming. This article offers an overview of the state-of-the-art advances and developments of the subject of synchronization on various complex networks, with emphasis on network synchronizability and performance.

Introduction

Many biological, social and technological systems can be properly described by complex networks with nodes representing individuals or organizations and edges characterizing the interactions among them [1,2,3,4,5]. One of the goals in the current studies on complex networks is to understand and explain how the topological properties of a network affect the behaviors of dynamical systems built upon the network. Typical examples include understanding how the topology of the Internet affects the spread of the computer viruses [6,7,8,9,10], how the structure of a power grid affects the cascading failures over time [11,12,13,14,15], how the connecting patterns of an intercommunication network affect its data traffic and dynamics [16,17,18,19,20], and so on.

Synchronous behaviors have been observed in various complex networks in nature and human society [23,24,25,26], and they have been studied for hundreds of years since the systematic investigation of pendulum synchrony by the great Dutch scientist Christian Huygens in 1665 [27].

To understand how network structure affects the synchronizability of a network not only has broad theoretical interest [28], but also has important practical value [29]. One typical case in point is the synchronicity of sen-

sors in biological neural networks, where neurons communicate with each other through synaptic junctions for which a mechanism called asynchronous release is important [30]. There are many careful studies about collective synchronization in the earlier literature, with a basic assumption that dynamical systems of coupled oscillators evolve either on regular networks [31,33,34] or on random networks [35,36]. However, the structures of most real-world networks are neither completely regular nor completely random, but rather, somewhere in between. Thus, it becomes important and even necessary to consider how network structure affects the synchronization process and the synchronizability of the dynamical systems on such networks. Recently, it has been found that networks with small-world effects and scale-free properties are quite different from, and oftentimes achieve synchronization more easily than, regular networks such as lattices [37,38,39,40,41,42,43,44].

The study of synchronization on complex networks has gone through several stages in the past decade, encompassing several important aspects of the subject: various synchronization phenomena on complex networks and their stability analysis, the relationships between structural ingredients and a network's synchronizability, the enhancement or reduction of network synchronizability, etc. The first two are quite well understood today while the last one will be further addressed in this article. First, some basic concepts about synchronization of networked dynamical systems and the associated stability analysis are introduced. Second, some intrinsic relations between network structure and synchronizability are discussed. Third, three types of methods, namely, regulating coupling patterns, modifying network structures, and designing output functions, are introduced for enhancing network synchronizability. Finally, some open questions are posed which are deemed significant for further studies of the important subject of complex network synchronization.

To proceed, some notations are introduced [5], among which three are most significant with respect to network synchronization: average distance L, clustering coefficient C, node-degree k_i of node i, and the corresponding probability density function of degree distribution $p(k)$.

In the past few years, by taking advantage of both high-speed computing power and the huge amount of real data available on the web, scientists were able to search and find some common statistical characteristics shared by many real-world networks. It is found that most real networks have a very small average distance, scaled approximately as $L \sim \ln N$, where N is the size of the network (i. e., the total number of its nodes), while their clustering coefficient is rather large, as compared with *random-graph networks*

(Erdös and Rényi [28]). A network having both of these two characteristics is referred to as a *small-world network*, described by Watts and Strogatz [21]. Moreover, the degree distributions of many real networks obey a power-law form $p(k) \sim k^{-\gamma}$, where $p(k)$ is the probability density function for the corresponding degree distribution, and γ is the power-law exponent (typically $2 < \gamma < 3$) [1,2,3]. The power-law distribution falls off much more gradually than an exponential one, allowing for a few nodes with very large degrees to exist. Networks with power-law degree distributions usually belong to the class of *scale-free networks*, characterized by Barabási and Albert [22].

Basic Concepts of Network Synchronization

A general model of coupled identical oscillators on a network can be described by [40,41]

$$\dot{x}_i = F(x_i) - \sigma \sum_{j=1}^{N} G_{ij} H(x_j), \quad i = 1, \dots, N, \quad (1)$$

where $\dot{x}_i = F(x_i)$ governs the dynamics of the ith oscillator, with state vector x_i; $H(x_j)$ is the output function; σ is the coupling strength; $G = [G_{ij}]$ is an $N \times N$ coupling matrix determined by the given coupling pattern among the N oscillators.

In the typical situation when the oscillators are symmetrically coupled, the coupling matrix G has the same form as the graph Laplacian L, i. e., $G = L$, with

$$L_{ij} = \begin{cases} k_i & \text{for } i = j \\ -1 & \text{for } j \in \Lambda_i \\ 0 & \text{otherwise}, \end{cases} \quad (2)$$

where k_i is the degree of node i and Λ_i is the set of its neighboring nodes. In this setting, L is symmetrical and semi-positive definite, and all the rows of L have a zero sum, so that its smallest eigenvalue λ_1 is always a single zero and all the other eigenvalues are strictly positive. Thus, the eigenvalues of L can be ranked as

$$0 = \lambda_1 < \lambda_2 \leq \lambda_3 \leq \cdots \leq \lambda_N.$$

For network (1), the synchronization manifold is an invariant manifold: $x_1 = x_2 = \cdots = x_N = s$, typically satisfies $\dot{s} = F(s)$ in engineering applications.

For a dynamical system, the so-called master stability function is usually defined to be the ratio of the largest Lyapunov exponent versus a connectivity parameter of the system [42,45]. For some dynamical systems, the master stability function is negative when $\lambda_2 > \alpha_1/\sigma$ for some
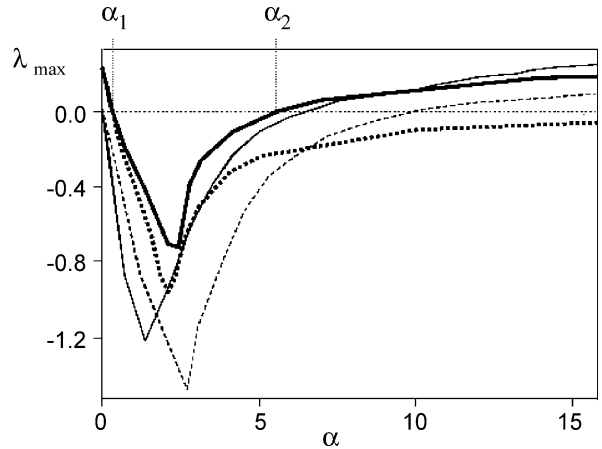
Synchronization Phenomena on Networks, Figure 1
Four typical master stability functions for coupled Rössler oscillators: chaotic (*bold curve*) and periodic (*regular curve*); with *y*-coupling (*dashed curve*) and *x*-coupling (*dotted curve*). The *vertical ordinate* shows the change of the largest Lyapunov exponent. Curves are all scaled for clearer visualization (after [42])

constant α_1. In this case, the largest Lyapunov exponent is negative, and consequently the network is synchronizable; moreover, the larger the λ_2 is, the better the network synchronizability will be [40,41].

For some other dynamical systems, the master stability function is negative only within a finite interval (α_1, α_2) [46], over which the largest Lyapunov exponent is negative [42,45], where α_1 and α_2 are constants. In this case, the network is synchronizable for some σ when the eigenratio $R = \lambda_N/\lambda_2$ satisfies $R < \alpha_2/\alpha_1$; moreover, a smaller R indicates a better network synchronizability.

The former case corresponds to networks for which the synchronized region is unbounded (the bold-dashed curve in Fig. 1), and the latter, bounded (the bold-solid curve and the two regular lines in Fig. 1) [42]. In both cases, the right-hand side of the above two inequalities depends only on the dynamics of each individual oscillator and the output function of the network, while the eigenvalue λ_2 and eigenratio R depend only on the Laplacian L. Therefore, the problem of synchronization can be divided into two parts: choosing suitable dynamics (including the aforementioned parameters and output function) and analyzing the eigenvalues of the Laplacian. In fact, these two cases can co-exist [32,101].

The same stability analysis can also be applied to some more complicated coupling patterns [40,41,42,45,47], including the case where G is non-diagonalizable (see Fig. 2 and [48]).

Network (1) has only identical oscillators, while in the real world parameter mismatch between oscillators is very

common, so that both the amplitudes and phases of different oscillators become different. However, quite often, only the frequencies of oscillations are of concern in some applications, while the amplitudes are not important. In such cases, phase synchronization is the topic for study, for which the *Kuramoto model* [49,50,51,52,53] is a representative platform.

In the Kuramoto model, oscillators run at arbitrary frequencies and they are coupled through a periodic (e. g., sine) function of their phase differences. More precisely, the model consists of a population of N coupled phase-oscillators $\theta_i(t)$ having natural frequencies ω_i distributed with a given probability density $g(\omega)$, governed by

$$\dot{\theta}_i = \omega_i - \sigma \sum_{j=1}^{N} G_{ij} \sin(\theta_i - \theta_j), \quad i = 1, \ldots, N. \quad (3)$$

To measure the synchronization phenomena, an order parameter M is introduced:

$$M \equiv \left[\left\langle \left| N^{-1} \sum_{j=1}^{N} e^{i\phi_j} \right| \right\rangle \right], \quad (4)$$

where ϕ is a function of θ, and $\langle \cdot \rangle$ and $[\cdot]$ denote the average over time and over different configurations, respectively.

Initially, each node is assigned a random phase. Without coupling, all the oscillators run independently and, at any time, the phases of the oscillators are distributed almost uniformly on the interval $[0, 2\pi]$, yielding $M = O(1/\sqrt{N})$. In this situation, the oscillators are generally not synchronized. With coupling, as the coupling strength gradually increases to beyond a certain threshold, interactions among oscillators become stronger and more inter-influential, which gradually dominate the individual self-oscillations. Eventually, collective synchronization of all oscillators emerges spontaneously. During this transition process, the order parameter M increases from 0 to 1.

Synchronizability Versus Structure

Previous studies have demonstrated that both scale-free and small-world networks are much easier to synchronize than regular lattices [37,38,39,40,41,42,43,44]. At this point, a natural question arises: what makes them easier to synchronize? An intuitive answer might be their average distance, which is much shorter than that of a regular network with the same size. However, after some systematic investigations on the relation between structural ingredients and the network synchronizability, Nishikawa et al. [54] found that as the network becomes more heterogeneous, i. e., the degree distribution becomes wider,
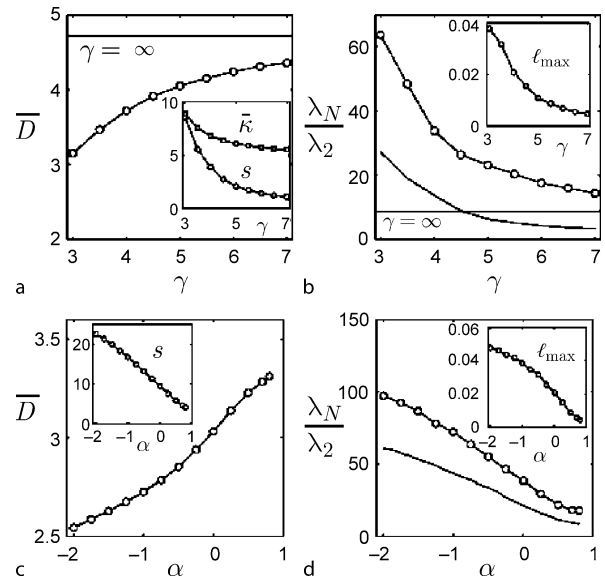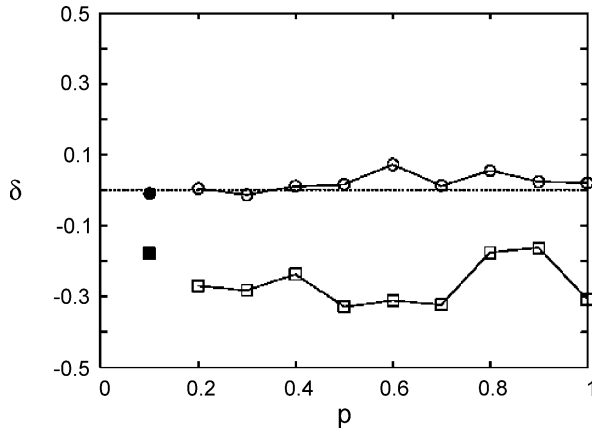

Synchronization Phenomena on Networks, Figure 2
Synchronization of scale-free networks. a, b the semi-random model; c, d the growing model with aging of nodes. The small insets are the responses of the indicated parameters with respect to the changing parameters γ or α under the same conditions (after [54])

a network can become less synchronizable even though its average distance becomes much shorter. Figure 2 gives two examples of this phenomenon. In a semi-random model [55], with the increase of the power-law exponent γ, which makes the network more homogeneous, the network average distance $\bar{D}$ becomes longer and the standard deviation of the degree distribution reduces (Fig. 2a and inset); meanwhile, the eigenratio λ_N/λ_2 of its Laplacian becomes smaller (Fig. 2b), indicating improvement of the network synchronizability. In a growing model of scale-free networks with aging nodes [56], it is also observed that as the average distance increases and the degree distribution becomes more homogeneous, the network gains a better synchronizability (Fig. 2c,d).

A heuristic exploration may be given: in a network with a heterogeneous degree distribution, a few "central" oscillators, which interact with a large number of other oscillators, tend to be overloaded by the traffic passing through them. When too many independent traffic signals with different phases and frequencies are traversing through a node at the same time, they cause congestion, leading to the reduction of network synchronizability. The same also happens to overloaded edges [54].

On the other hand, based on experience with WS small-world networks, Hong et al. [57] concluded that the

Synchronization Phenomena on Networks, Figure 3
Behavior of the difference δ of the eigenratio in a WS network
with rewiring probability p (after [57])

Synchronization Phenomena on Networks, Figure 4
Sketch of maps of the random interchanging algorithm (after [62])

maximal node betweenness [58,59,60] is a good indicator for network synchronizability: the smaller, the better, and vice versa. To confirm their observation, they calculated the difference of the eigenratio before and after the removal of a node from a WS network [21]. Figure 3 plots the difference $\delta \equiv (\lambda_N/\lambda_2)_{\text{after}} - (\lambda_N/\lambda_2)_{\text{befor}}$. The reduction of the ratio is brought about by the removal of the node with the maximal betweenness (empty squares in the figure). In comparison, random removal of a node makes the eigenratio almost unchanged (empty circles in the figure). This implies that the node with the maximal betweenness plays an important role in determining the synchronizability of the network. However, for scale-free networks, this "maximal betweenness indicator" may not work, as pointed out in [61] with a counterexample given in [62].

In the above studies, a network is usually modified in order to see how the synchronizability changes as the network structure varies. It is worth emphasizing that during the modification process all the topological ingredients [5] have been changed at the same time, therefore it is impossible to obtain any accurate relation between one particular ingredient and the network synchronizability. Knowing this problem, by using the edge-exchange operation [63,64], Zhao et al. [62] derived some fairly accurate relations between the synchronizability and the average distance as well as the heterogeneity of the degree distribution, on small-world and scale-free network models. Figure 4 presents a sketch of maps of their random interchanging algorithms. The algorithmic operations will change only the network average distance while keeping the degree of each node unchanged. Thus, the relations between the two concerned ingredients can be investigated
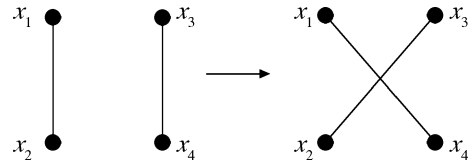
separately. Extensive simulations have verified that either shortening the average distance or lowering the heterogeneity may lead to a better synchronizability, but only their combination can always ensure that the network will synchronize easily.

McGraw and Menzinger [65] investigated the relations between the clustering coefficient and network synchronizability, and concluded that for both random-graph and scale-free networks, increasing the clustering coefficient hinders global synchronization if the coupling strength is strong, but it promotes the synchronization of scale-free networks when the coupling strength is weak. Figure 5 shows this phenomenon. The main reason is that the clusters around the hub-nodes promote the formation of frequency-synchronized clusters, but they will inhibit the synchronization of the network as a whole. The early hub synchronization accounts for the slightly enhanced order parameter when the coupling is weak [65,66]. This analysis is based on non-identical oscillators in the Kuramoto model. On the other hand, by means of master stability analysis, Wu et al. [67] reported a negative correlation between the clustering coefficient and synchronizability through a scale-free network model with a tunable clustering coefficient [68].

Besides the main focus on small-world effects and scale-free properties, as described by the clustering coefficient, average distance and degree distribution, some further studies on the effects of other topological ingredients on network synchronization have also been reported, particularly the degree-degree correlation. A network is said to show *assortative* (or *disassortative*) *mixing*, if the nodes having many connections tend to connect to other nodes with many (or few) connections. The extent of this degree-degree correlation can be measured by the Pearson coefficient [69]: its positive (or negative) value indicates assortative (or disassortative) mixing. Di Bernardo et al. found that disassortative networks generally have a better synchronizability than the assortative ones [70,71]. However, later works [72,73] show that the degree distribution, coupling pattern, and degree-degree correlation among the nodes compete with each other in an intrinsic manner,
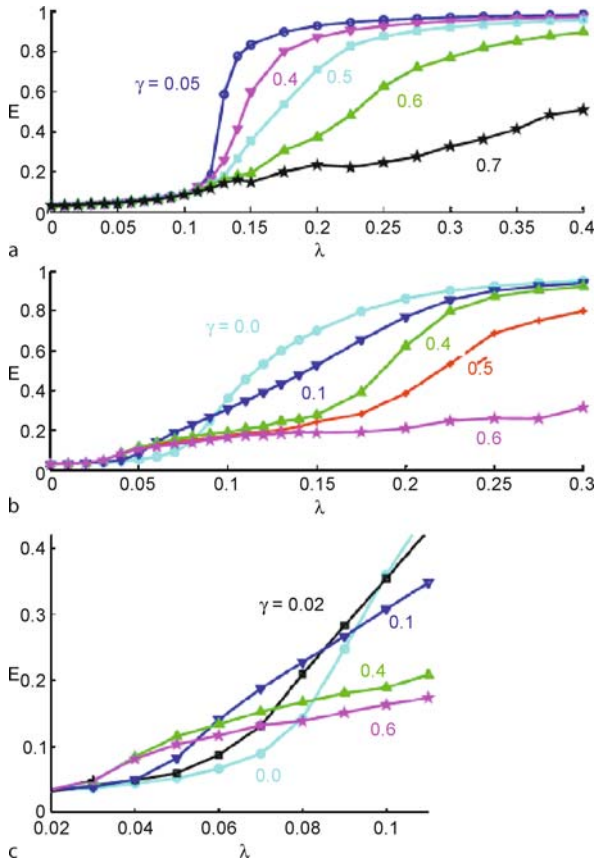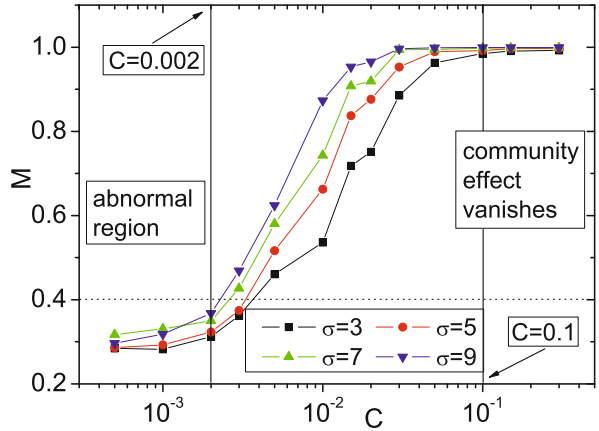
Synchronization Phenomena on Networks, Figure 5
Order parameter *M* vs coupling strength λ, for different values of the clustering coefficient γ. **a** Poisson degree distribution. **b, c** Power-law degree distribution. **c** A close-up of the transition region, showing that increase of the clustering coefficient leads to an advanced (lower-λ) transition (after [65])

Synchronization Phenomena on Networks, Figure 6
Order parameter *M* vs. community strength *C* for different values of the coupling strength σ (after [76])

thereby together determining the network synchronizability. That is, for one coupling pattern, disassortative mixing may predict better synchronizability, while for another coupling pattern, the result can be the opposite.

As we gain more knowledge of various network structures, more attention is paid to the effects of local structures of complex networks on their global behaviors and dynamics. Huang et al. [74] found that in complex networks with prominent clusters, the synchronizability is determined by the interplay between intercluster and intracluster edges: a network is mostly synchronizable when the numbers of the two types of edges are approximately equal. If not equal, for example as the number of intracluster edges increases, an abnormal synchronization phenomenon appears: although the network average distance becomes smaller, the network synchrony is weakened or even destroyed.

Furthermore, the synchronization phenomenon of a complex network with a community structure has also been discussed. Qualitatively, a *community* is defined as a subset of nodes within a network with the property that the connections among the nodes therein are denser than those within the other parts of the network [75]. Zhou et al. studied phase synchronization in a network with a community structure [76]. Defining the edges connecting two nodes in one community as *internal edges*, and those connecting nodes between two communities as *external edges*, the ratio of the number of external edges to the number of internal edges can be used to characterize the strength of the community structure, denoted by *C*. Clearly, a smaller *C* corresponds to sparser external edges thus a more prominent community structure. Figure 6 shows the relationship between the order parameter *M* and the community strength *C* for different coupling strengths σ. It is found from Fig. 6 that a strong community structure will hinder global synchronization no matter what the coupling strength is, but this effect will vanish when the fraction of external connections exceeds 0.1.

Using a modified simulated annealing algorithm, Donetti et al. [77] generated an entangled network with optimal synchronizability. These kinds of networks are shown to have an extremely homogeneous structure: distributions of node degrees, distances, betweenness, and loops are all very uniform. Also, these networks are characterized by short average distances and large loops, with no well-defined community structures. In the approach of [77], rewiring is applied, i. e., at each time step, the number of rewiring trials is randomly extracted from an exponential distribution. Except for rewiring which reduces or increases the eigenratio, and except for operations that
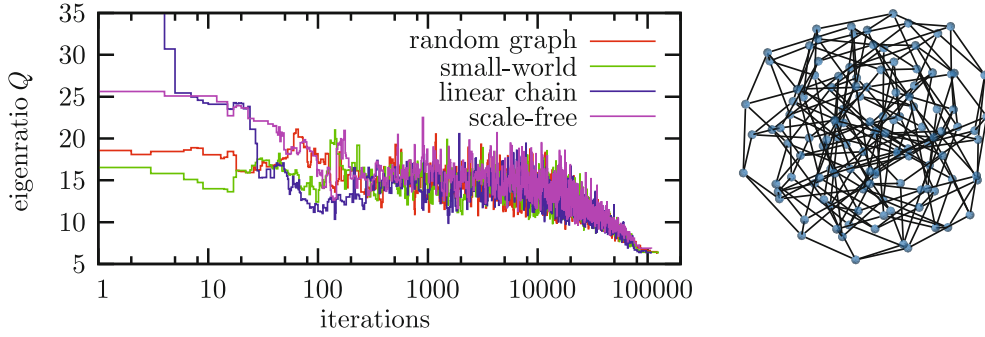
Synchronization Phenomena on Networks, Figure 7
Eigenratio Q as a function of the number of algorithmic iterations. Starting from different initial configurations, all the networks are converted via iterations to *entangled networks* (after [77])

disconnect the network, for different initial configurations the optimization process will always lead to the same optimal result. Figure 7 shows the changes of the eigenratio in the optimizing process and the resultant network configuration.

Enhancing Network Synchronizability

With a clearer understanding of the relations between the network structure and synchronizability, a natural question about how to enhance the network synchronizability is in order. Some effective synchronizability-enhancement methods are introduced in this section.

Coupling Pattern Regulation

In general, scale-free networks are much harder to synchronize than random networks with the same size and the same average degree. One reason is that in scale-free networks, there are some "central" oscillators that interact with a large number of other nodes [54]. Thus, when too many independent signals with different phases and frequencies are traversing through a "central" oscillator at the same time they may have conflicts, thereby causing traffic congestion. Hence, generally speaking, the more heterogeneous the degree distribution, the more difficult for the network to synchronize. It is also known that in scale-free networks, when the oscillators are coupled symmetrically, oscillators with larger degrees usually approach the final synchronized state first, and then the others with smaller degrees synchronize to them gradually [65]. Therefore, when the oscillators are coupled asymmetrically, if the coupling strength from the "central" oscillators to the other nodes are stronger than the reverse, the network will synchronize much easier and faster.

Based on this idea, Motter, Zhou and Kurths [78,79,80] proposed a new coupling pattern, which we will call the

MZK pattern, which can sharply improve network synchronizability. After that, quite a few methods for regulating coupling patterns are brought forward to improve network synchronizability, some static and some dynamic.

Static Coupling Patterns

In static coupling patterns, the elements of the coupling matrix are formulated based on the MZK pattern, as

$$G_{ij} = L_{ij}/k_i^\beta \,, \tag{5}$$

where β is a tunable parameter. The coupling is weighted when $\beta \neq 0$, and unweighted when $\beta = 0$. In spite of the asymmetry of this coupling matrix G, it can be proved that all the eigenvalues of G are nonnegative reals with only one eigenvalue being zero if the network is connected. Rewrite Eq. (5) as

$$G = D^{-\beta} L \,, \tag{6}$$

where $D = \mathrm{diag}(k_1, \ldots, k_N)$ is a diagonal matrix and L is the Laplacian. From the identity

$$\det(D^{-\beta} L - \lambda I) = \det(D^{-\beta/2} L D^{-\beta/2} - \lambda I) \,, \tag{7}$$

where I is the $N \times N$ identity matrix, one can prove that the spectrum of G is the same as that of the following symmetric matrix:

$$H = D^{-\beta/2} L D^{-\beta/2} \,. \tag{8}$$

Similarly to the case of matrix G, if the network is connected then all eigenvalues of H other than the single $\lambda_1 = 0$, are positive. With $\beta = 1$, the matrix H is a normalized Laplacian. Thus, if the network is connected and $N \geq 2$, then

$$0 < \lambda_2 \leq N/(N-1) \,, \quad 2 \leq \lambda_N \leq N/(N-1) \,. \tag{9}$$
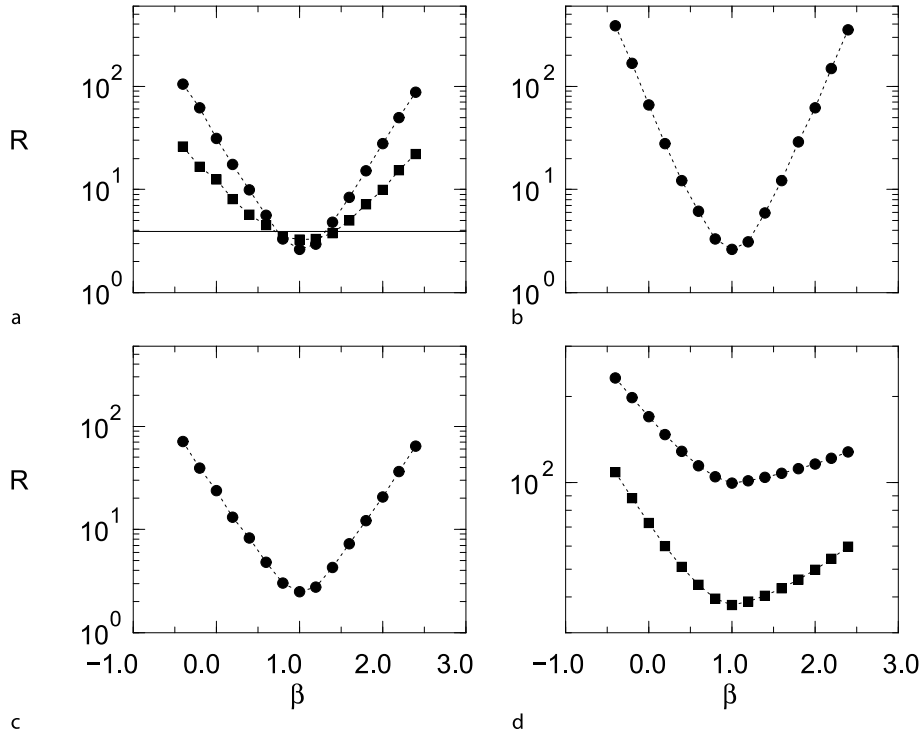
Synchronization Phenomena on Networks, Figure 8
Eigenratio R as a function of β for four kinds of complex networks specified in [78]. For each model, the synchronizability peaks at $\beta = 1.0$ (after [78])

Figure 8 shows the changes of the eigenratio R with the parameter β in four kinds of complex networks specified in [78]. It can be seen that the eigenratio R has a well-defined minimum at $\beta = 1$ in all cases. Mathematically, this means that the best results are obtained when the matrix D has a square-root. It is also clear that the more heterogeneous the network is, the more prominent the minimum of the eigenratio R becomes.

By explicitly relating the asymmetry in the connections to an age order among different nodes, Hwang et al. [81] found that age-ordered networks provide a better propensity for synchronization. The main reason is that an older node becomes weaker, therefore more easily influenced by other nodes. In this coupling pattern, the off-diagonal entries of the zero-row-sum coupling matrix G are

$$G_{ij} = -a_{ij} \frac{\Theta_{ij}}{\sum_{j \in \Lambda_i} \Theta_{ij}} , \qquad (10)$$

where a_{ij} are the elements of the adjacency matrix A ($a_{ij} = 1$ if nodes i and j are connected, and $a_{ij} = 0$ otherwise), and $\Theta_{ij} = (1 - \theta)/2$ (or $\Theta_{ij} = (1 + \theta)/2$) for $i > j$ (or $i < j$). The parameter $\theta \in (-1, 1)$ governs the coupling asymmetry in the network: the limit $\theta \to -1$ (or $\theta \to 1$) gives a unidirectional coupling, where the old (or

young) nodes drive the young (or old) ones. When $\theta = 0$, the coupling pattern degenerates to the MZK pattern at $\beta = 1$.

For a generic θ, the spectrum of the coupling matrix G is in the complex plane and the complex eigenvalues appear in pairs of complex conjugates ($\lambda_1 = 0$; $\lambda_\ell = \lambda_\ell^r + j\lambda_\ell^i$, $\ell = 2, \ldots, N$). It can be proved that (i) $0 < \lambda_2^r \leq \cdots \leq \lambda_N^r \leq 2$, and (ii) $|\lambda_\ell^i| \leq 1, \forall \ell$. The best propensity for synchronization is then ensured when both the ratio $\lambda_N^r / \lambda_\ell^r$ and $M \equiv \max_\ell\{|\lambda_\ell^i|\}$ are simultaneously made as small as possible.

In scale-free network models, the age of a node can be denoted by the time when it is being added to the network. The class of scale-free networks under study is generated from the Barabasí–Albert model [82,83]. For comparison, a highly homogeneous random network with an arbitrary initial age ordering is considered, with the average degree being equal to that of the scale-free network. Figure 9 shows the variation of the synchronizability of the two networks versus the parameter θ. For the random network, symmetric coupling makes the ratio $\lambda_N^r / \lambda_2^r$ smallest, while for the scale-free model, the propensity for synchronization is better (or worse) when $\theta \to -1$ (or $\theta \to 1$). As for M, there are only very small differences between
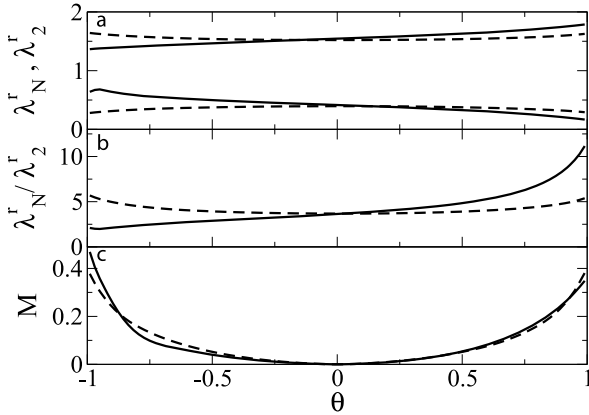
Synchronization Phenomena on Networks, Figure 9
a λ_N^r and λ_2^r, **b** λ_N^r/λ_2^r, and **c** M, vs. θ, for a scale-free network ($m = 5$ and $B = 0$, *solid curves*) and random network (*dashed curves*) (after [81])

the scale-free and the random-network models. Thus, it is concluded that in scale-free networks, the network synchronizability is enhanced when the dominant coupling direction is from older to younger nodes [84].

Taking the edge-weights into account, Chavez et al. [85,86] investigated the propensity for synchronization of some weighted complex networks, where the weight in an arbitrary edge, ℓ_{ij}, is defined as its traffic load [87], which quantifies the traffic of shortest paths which make use of that edge. In this coupling pattern, the off-diagonal entries of the zero-row-sum coupling matrix G are

$$G_{ij} = -\frac{\ell_{ij}^\alpha}{\sum_{j\in\Lambda_i}\ell_{ij}^\alpha}\,, \tag{11}$$

where α is a tunable parameter, and ℓ_{ij} is the load of the edge connecting nodes i and j.

Although G is asymmetric for all α, just like the MZK pattern, it can be proved that all its eigenvalues are non-negative reals with only one zero eigenvalue if the network is connected. The case of $\alpha = 0$ corresponds to the best synchronizability condition for the MZK pattern. From Eq. (11), it can be seen that in the limit of $\alpha = +\infty$ (or $\alpha = -\infty$) only the edges with the largest (or smallest) loads ℓ_{ij} are selected as the incoming edges for each node i. Therefore, this generates a network with at least N directed edges, which can be either connected or disconnected. In the connected (or disconnected) case, the ratio λ_N/λ_2 will be equal to 2 (or $+\infty$), thus yielding a very strong (or weak) condition for synchronization.

Figure 10a shows the logarithm of λ_N/λ_2 in the parameter space (α, B) for the above-discussed model [82,83]. Parameter B is used to regulate the heterogeneity of the
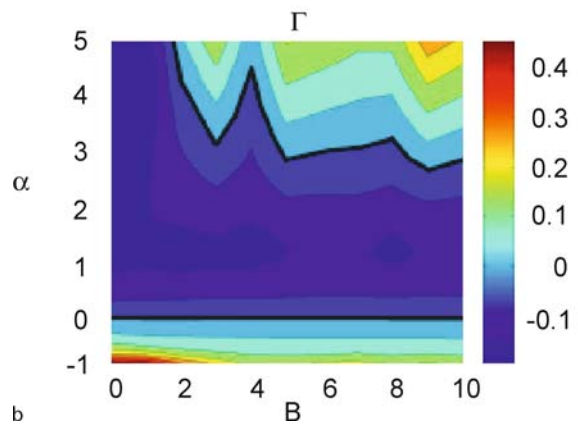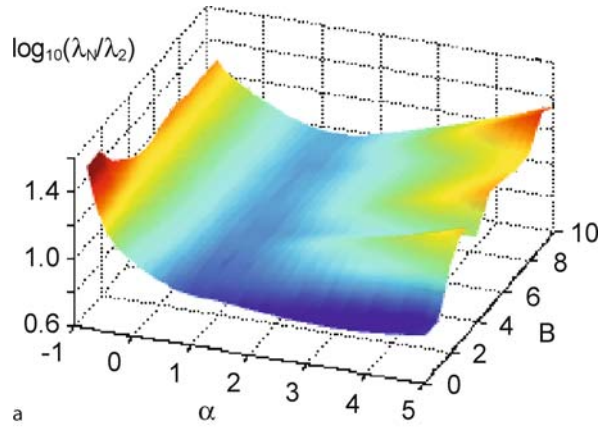
Synchronization Phenomena on Networks, Figure 10
a λ_N/λ_2 for scale-free networks vs. the parameter space (α, B). **b** $\Gamma = \log(\lambda_N/\lambda_2) - [\log(\lambda_N/\lambda_2)]_{\alpha=0}$ vs. (α, B). The domain with $\Gamma < 0$ is outlined by the *black contours* drawn (after [85])

degree distribution. It can be observed that the surface of λ_N/λ_2 has a prominent minimum when $\alpha \simeq 1$ for all values of B above a given threshold $B_c > 0$, which means that the weighting procedure based on edge loads always enhances the network propensity for synchronization. The quantity $\Gamma = \log(\lambda_N/\lambda_2) - [\log(\lambda_N/\lambda_2)]_{\alpha=0}$ shown in Fig. 10b may be used to quantify the synchronizability enhancement.

The coupling patterns proposed by both Hwang et al. [81] and Chavez et al. [85,86] can enhance the propensity for network synchronization. The former works well only for age-ordered networks, while the latter requires the knowledge of the load on each edge of the whole network. Therefore, a general coupling pattern using only local information would be very desirable. Based on the idea that different nodes should play different roles in a network, Zhao et al. [73] proposed a coupling pattern which
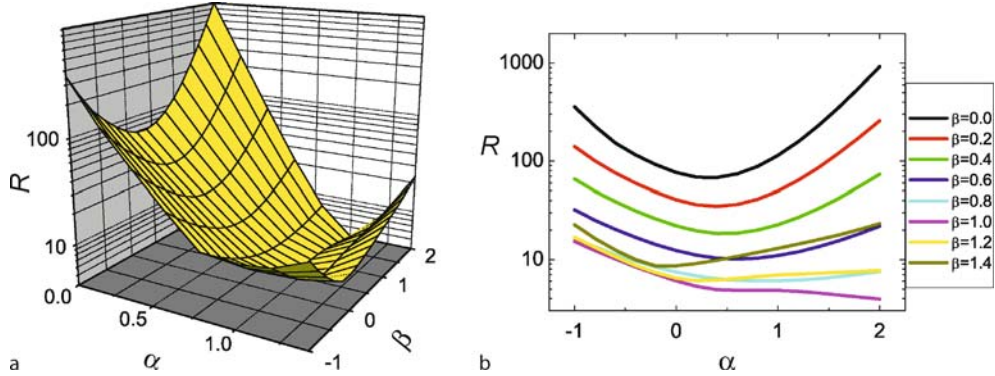
Synchronization Phenomena on Networks, Figure 11
a Eigenratio R in the parameter plane (α, β). **b** R vs. α for different values of parameter β (after [73])

requires only the degrees of neighboring nodes. The coupling matrix G of this pattern is given by

$$G_{ij} = \begin{cases} -k_j^\alpha/S_i^\beta & \text{for } j \in \Lambda_i \\ S_i/S_i^\beta & \text{for } i = j \\ 0 & \text{otherwise,} \end{cases} \qquad (12)$$

where $S_i = \sum_{j \in \Lambda_i} k_j^\alpha$. When $\alpha = \beta = 0$, this coupling pattern degenerates to the symmetric coupling pattern [45], where the case of $\alpha = 0$ corresponds to the MZK pattern [78] and the case of $\beta = 1$ is equivalent to the one introduced in [80] (see Eq. (15) in [80] for more details). Although this G is asymmetric for all α with $\beta \neq 0$, it can also be proved that all its eigenvalues are non-negative reals with only one zero eigenvalue, if the network is connected. Figure 11 shows some simulation results. From the figure, it can be concluded that there is always some parameter region in which the eigenratio R is smaller than that of the symmetrically coupled case ($\alpha = \beta = 0$) and that of the optimal case with the MZK pattern ($\alpha = 0$ and $\beta = 1$).

From the viewpoint of gradient fields, Wang et al. [88] also derived a coupling pattern that has the same configuration as Eq. (12) with $\beta = 1$.

Dynamic Coupling Patterns

The coupling patterns discussed above are all based on a network having a fixed structure which remains unchanged throughout the synchronizing process.

Zhou et al. [89] investigated synchronization in a scale-free network of chaotic oscillators, where the coupling strength of a node develops adaptively according to the local synchronizing property between the node and its neighbors. In this coupling pattern, the off-diagonal entries of the zero-row-sum coupling matrix G are

$$G_{ij} = -a_{ij}W_{ij}, \qquad (13)$$

where $W_{ij} > 0$ is the coupling strength from node j to node i if they are connected. Here, suppose that the strength between node i and all its k_i neighbors increases uniformly among the k_i connections, in order to suppress its difference Δ_i from the mean activity of its neighbors; namely,

$$G_{ij}(t) = -a_{ij}V_i(t), \quad \dot{V}_i = \gamma\Delta_i/(1 + \Delta_i), \qquad (14)$$

where $\Delta_i = |H(\boldsymbol{x}_i) - (1/k_i)\sum_j a_{ij}H(\boldsymbol{x}_j)|$, and $\gamma > 0$ is the adaptation parameter. It is clear that, in this adaptive coupling scheme, the input weight ($W_{ij} = V_i$) and the output weight ($W_{ji} = V_j$) of node i are generally asymmetrical.

Next, synchronization of a network of coupled Rössler oscillators and a chaotic foodweb model on Barabási–Albert scale-free networks are considered, and two cases of unbounded and bounded stability zones are investigated, respectively. When the stability zone is unbounded, the transition to synchronization is shown in Fig. 12a. Starting from random initial conditions on the chaotic attractors, the local synchronization difference $\Delta \gg 1$, and the input weights of each node, both increase uniformly on the whole network, i. e., $W_{ij} = V_i(t) \approx \gamma t$ (Fig. 12a, inset). After a short period of time, the weights V_i of different nodes develop at different rates and then converge to different values $\tilde{V}_i$. The input weight is smaller on average for nodes with larger degrees k_i (Fig. 12b). Here, the synchronization error is measured by averaging all local errors over the nodes: $E(t) = \langle|\boldsymbol{x}_i - \langle\boldsymbol{x}_i\rangle|\rangle$.

The dependence of the input weight of a node on its degree follows a power law,

$$V(k) \sim k^{-\theta}, \qquad (15)$$
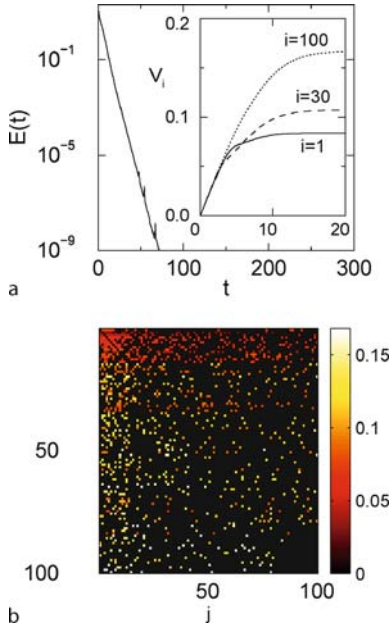
Synchronization Phenomena on Networks, Figure 12
a Transition to synchronization in an adaptive network of Rössler oscillators, indicated by the (averaged) synchronization error $E(t) = \langle |x_i - \langle x_i \rangle| \rangle$. *Inset*: the input strength $V_i(t)$ vs. time over three nodes. **b** The weighted coupling matrix $\tilde{G}$ crystallized after the adaptation (for the foodweb model) (after [89])

with exponent $\theta = 0.48 \pm 0.01$ for both oscillator models. Importantly, this scaling is also robust to the variation of network parameters, such as the minimal degree M (Fig. 13b), which should not be confused with the order parameter M elsewhere, the system size N (Fig. 13c), and the orders of magnitudes of the adaptation parameter γ (Fig. 13d).

When the stability zone is bounded, synchronization can always be achieved by the adaption mechanism of Eq. (14) if $\gamma \leq \gamma_c$ for a threshold γ_c somewhat depending on N and the oscillator dynamics. The two resulting weighted networks display the same power-law behavior as in Eq. (15), but with different exponents: $\theta = 0.54 \pm 0.01$ (Rössler oscillator) or $\theta = 0.36 \pm 0.01$ (foodweb). The eigenratio R for the weighted networks, after the adaptation, and for the unweighted networks (symmetric coupling) is calculated as a function of N (Fig. 14a), and as a function of the ratio S_{max}/S_{min} (Fig. 14b), where S_{max} and S_{min} are the maximum and minimum intensities of the variable coupling strengths of the model. Clearly, this adaptive coupling scheme is more effective than symmetric coupling for network synchronization.

Huang [90] investigated another adaptive coupling pattern, in which a node is coupled with its neighbors

non-uniformly through different coupling strengths, and showed that they have better synchronizability than other networks with symmetric coupling patterns.

In all the coupling patterns discussed above, whether the coupling pattern is static or dynamic, only the coupling strength is tunable while the connectivity matrix always remains unchanged. However, as is intuitively clear, network synchronizability can also be significantly improved by evolving the graph topology giving rise to a time-varying connectivity matrix. This has been recently confirmed by Boccaletti et al. [91].

It has been shown [91] that to make a network synchronizable, either the coupling matrix $G(t) = G$ remains unchanged, or if starting from an initial wiring condition $G(0) = G_0$, the coupling matrix $G(t)$ commutes at any time with G_0, i.e., $G_0 G(t) = G(t)G_0, \forall t$. At any time, a zero-row-sum symmetric commuting matrix $G(t)$ can be constructed, as

$$G(t) = V \Lambda(t) V^T , \qquad (16)$$

where $V = \{v_i, \ldots, v_N\}$ is an orthogonal matrix with columns being the eigenvectors of G_0, and $\Lambda(t) = \mathrm{diag}[0, \lambda_2(t), \ldots, \lambda_N(t)]$ with $\lambda_i(t) > 0, \forall i > 1$. This set of matrices is referred to as the dissipative commuting set of $G(0)$. A condition to ensure the network synchronization will be stable is

$$S_i = \lim_{T \to \infty} \frac{1}{T} \int_0^T \Lambda_{max}(\sigma \lambda_i(t')) \mathrm{d}t' < 0 \quad \forall i \neq 1, \quad (17)$$

where $\Lambda_{max}(\sigma \lambda_i)$ is the maximal transversal (conditional) Lyapunov exponent along the direction of the ith eigenvector, and S_i is its time average. Hence, it does not require $\Lambda_{max}(\sigma \lambda_i(t)) < 0$ at all times. One can even construct a commutative evolution such that at each time there exists one eigenvalue λ_i for which $\Lambda_{max}(\sigma \lambda_i(t)) > 0$, and yet obtain a stable synchronization manifold. Thus, interestingly, synchronization in a dynamical network can be achieved even in the case where each individual commutative graph does not give rise to synchronized behavior.

Modifications of Network Structures

It is well known that the synchronizability of a dynamical network is determined simultaneously by the network coupling pattern, the dynamical characteristics of the oscillators on its nodes, and the network structure. In the above, several cases with variable coupling patterns have been discussed. For some real-world networks, however, the coupling pattern cannot be modified at will. Thus, if the dynamics of the oscillators are given and fixed, and
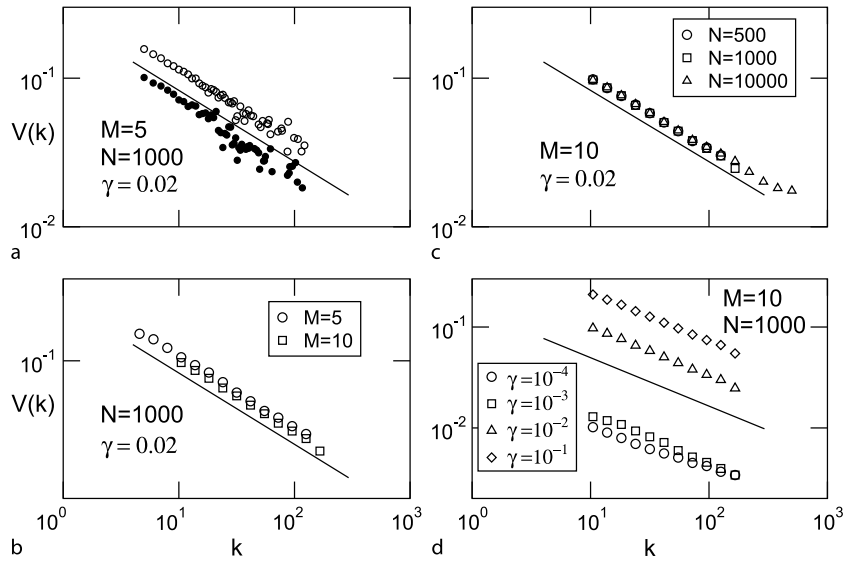
Synchronization Phenomena on Networks, Figure 13
Average input weight $V(k)$ of nodes with degree k as a function of k for a network of Rössler oscillators (*empty circles*) and the food-web model (*filled circles*) (**a**), and its dependence on various parameters, M (**b**), N (**c**), and γ (**d**), where the M should not be confused with the order parameter M elsewhere (after [89])
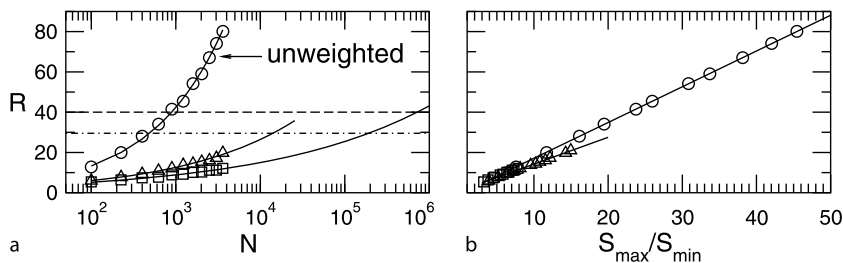
Synchronization Phenomena on Networks, Figure 14
Eigenratio R as a function of N (**a**), and S_{max}/S_{min} (**b**). The networks are synchronizable if $R < R_\epsilon$ in **a**, Rössler oscillators (*squares*), $R_\epsilon = 40$ (*dashed curve*), foodweb model (*triangles*), $R_\epsilon = 29$ (*dashed-dotted curve*) (after [89])

if the coupling patterns cannot be changed, then the only way to enhance the network synchronizability is to make a change to the network structure.

There are some effective techniques to enhance the network synchronizability by modifying the network structure, as further discussed below in the rest of this section.

Reducing Maximal Betweenness

In scale-free networks, the average distance is often very short while the node-degree and node-betweenness distributions are both quite broad. The bottleneck for the network synchronizability seems to be the maximal node betweenness [57]. In order to reduce the node betweenness of the hubs, Zhao et al. [92] suggested a method of struc-

tural perturbations. Specifically, for a hub x_0, $m - 1$ auxiliary nodes, labeled as $x_1, \ldots, x_{m-1}$, are added around it. These m nodes are fully connected together. Then, all the edges incident from x_0 are re-distributed to all the nodes x_i (including x_0 itself), $i = 0, 1, \ldots, m - 1$. After this process, the betweenness of x_0 is divided into m almost equal parts associating with these m nodes. This process is called m-division. A sketch map of a 3-division process on node x_0 is shown in Fig. 15.

Due to the huge sizes of many real-life networks, it is usually impossible to obtain the node betweenness from a complex network. Fortunately, studies have shown that there exists a strongly positive correlation between the node-degree and the node-betweenness in Barabasí–Albert networks and some other heterogeneous networks [87,93]. That is, a node with larger degree has
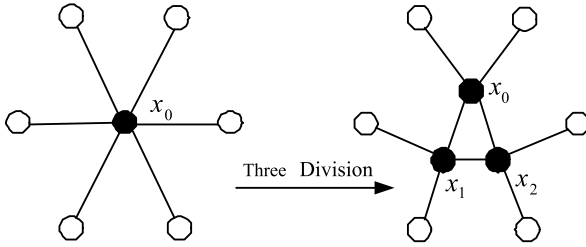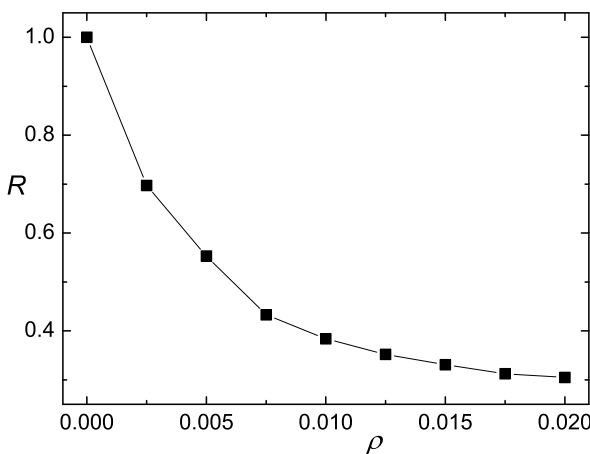
Synchronization Phenomena on Networks, Figure 15
Sketch map for the 3-division process on x_0. The *solid circle* on the *left* is the node x_0 with degree 6. After the 3-division process, this x_0 is divided into 3 nodes, x_0, x_1 and x_2, which are fully connected. The six edges incident from x_0 are then re-distributed to all the three nodes (after [92])

higher node-betweenness statistically. Therefore, for practical reasons, it can be assumed that nodes with higher betweenness are those with larger degrees in Barabási–Albert networks.

To further explore how the structural perturbations affect the network synchronizability, the eigenratios before and after the m-division process were compared in [92] for a Barabási–Albert scale-free network with the coupling matrix being Laplacian. For use in the rest of the article, we define a characteristic value $R = r'/r$, in which r and r' are the eigenratios before and after the division, respectively. Figure 16 shows the correlation between R and the probability ρ of the divided nodes. It is clear that even the m-division of a tiny fraction of nodes can sharply enhance network synchronizability.

Shortening the Average Distance

Zhou et al. [94] investigated the synchronizability of a network model named *crossed double cycles* (CDCs). They not only clarified the relationship between average distance and network synchronizability, but also provided a possible way to make a network more synchronizable.

In the language of graph theory [95,96,97], a cycle C_N denotes a network consisting of N nodes (vertices) x_1, $\dots$, x_N. These N nodes are arranged in a ring, and the nearest two nodes are connected to each other. Thus, C_N has N edges connecting the nodes $x_1 x_2, x_2 x_3, \dots,$ $x_{N-1} x_N, x_N x_1$. The set of all such CDCs, denoted by $G(N, m)$, can be constructed by adding two edges, called crossed edges, to each node in C_N. The two nodes connecting by a crossed edge have distance m within C_N. For example, the network $G(N, 3)$ can be constructed from C_N by connecting $x_1 x_4, x_2 x_5, \dots, x_{N-1} x_2, x_N x_3$ together. A sketch map of $G(20, 4)$ is shown in Fig. 17 for illustration.

Figure 18 shows how the average distance L affects the network synchronizability (measured by the characteristic value R). It is clear that the network synchronizability is very sensitive to the average distance: as L increases, R sharply spans more than three magnitudes. And the network synchronizability is remarkably enhanced by reducing L. When the crossed length m is not too small or too large (compared to N), networks with the same average distance have approximately the same synchronizability,
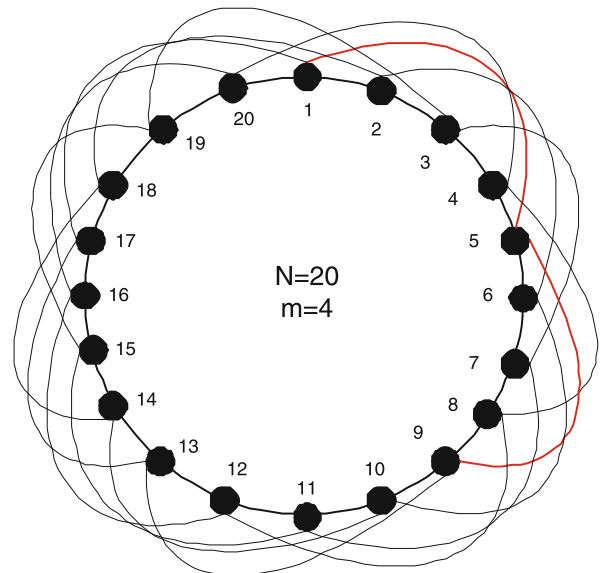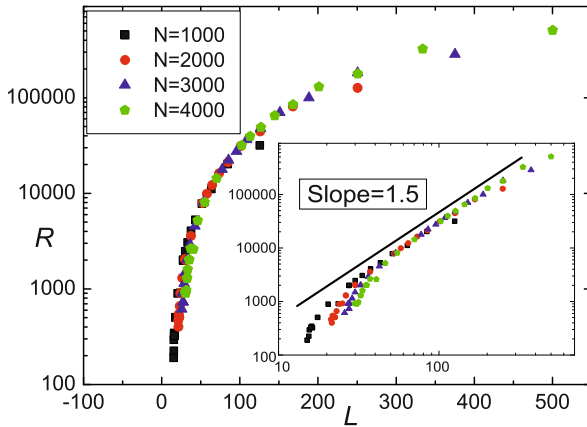

Synchronization Phenomena on Networks, Figure 16
Behavior of value R vs. the fraction of divided nodes ρ. As the number of divided nodes increases, R is reduced, leading to better synchronization (after [92])

Synchronization Phenomena on Networks, Figure 17
Sketch map of $G(20, 4)$ (after [94])

Synchronization Phenomena on Networks, Figure 18
Characteristic value R vs. average distance L of CDCs. The *black squares*, *red circles*, *blue triangles* and *green pentagons* represent the cases of $N = 1000$, 2000, 3000 and 4000, respectively. The *inset* shows the same data in log-log plot, indicating that the characteristic value R approximately obeys a power-law form $R \sim L^{1.5}$. The *solid line* has slope 1.5, for comparison (after [94])

Synchronization Phenomena on Networks, Figure 19
Changes of the synchronizability as a function of the proportion of cut edges N_{cut}/N for different values of the average distance (after [99])
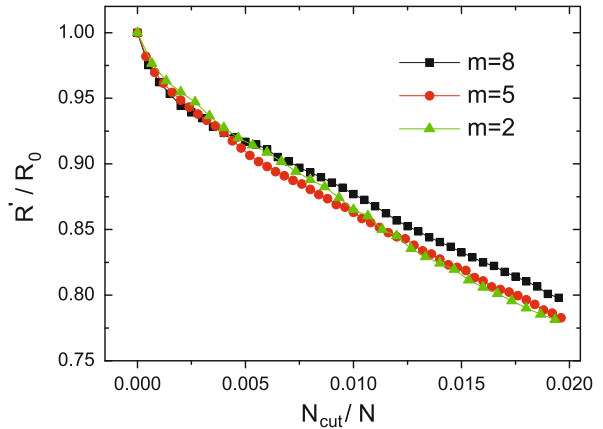
regardless of the network sizes. More interestingly, the numerical results show that the characteristic value R approximately obeys a power-law form, as $R \sim L^{1.5}$ (inset of Fig. 18).

Decoupling Nodes by Removing Heavily-Loaded Edges

In the synchronization process, not only hubs may be the bottlenecks but some edges with large loads may also limit the network synchronizability. Yin et al. [99] found that a scale-free network can become more synchronizable after some of its heavily-loaded edges have been removed. To reduce the computational cost, they used local information to approximately rank the edges, according to the values of $k_i \times k_j$, where i and j denote two adjacent nodes connected by an edge. Subsequently, at each time step, an edge with the highest rank is removed, i. e., the two nodes are decoupled at both sides of their connecting heavily-loaded edge. After this operation, the characteristic value is decreased, as shown by Fig. 19.

Designing the Output Function

Very recently, the relationship between graph theory and network synchronizability received some special attention [100]. For example, Duan et al. [101,102,103] found that for networks with disconnected complementary graphs, adding edges will often increase their synchronizability. The complementary graph of a given graph G is

defined to be the graph consisting of all the nodes of G and all the edges that are not in G.

In addition, they found [101,102] that when the couplings between nodes are symmetric, an unbounded synchronized region is always easier to analyze than a bounded synchronized region (see Sect. "Basic Concepts of Network Synchronization" to recall their definitions). Therefore, to effectively enhance network synchronizability, they presented a design method for the output function (i. e., H in network (1), or the inner linking matrix in the linear coupling case), such that the resultant network has an unbounded synchronized region, for the case where the synchronous state is an equilibrium of the network.

If the synchronous state is an equilibrium, then both $DF(s(t))$ and $DH(s(t))$ in network (1), as discussed in Sect. "Enhancing Network Synchronizability" (part B), reduce to constant matrices, denoted by F and H, respectively. The synchronized region is the stability region of the matric pencil $F + \alpha H$ with respect to parameter α. It can be proved that there exists a matrix H of rank 1 (meaning that only one component in each state vector is used for coupling), such that the stability region is unbounded. The method for obtaining the desired output function is outlined below: first, take a column vector b such that (F, b) is stabilizable [104]; then, find a matrix $P = P^{\mathrm{T}}$ such that $FP + PF^{\mathrm{T}} - 2bb^{\mathrm{T}} < 0$; consequently, taking $k = b^{\mathrm{T}}P^{-1}$ leads to the stability of $F - \alpha bk$ for all α in the unbounded region; finally, $H = bk$ is the matrix to be found.

For illustration, synchronization of a simple 6-node network (shown in Fig. 20) is studied, where each node
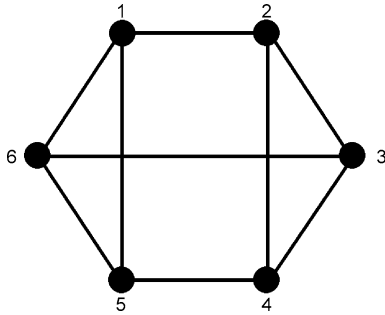
Synchronization Phenomena on Networks, Figure 20
A network of 6 nodes (after [101])

is located with a third-order smooth Chua's circuit [105]. At first, arbitrarily take the output function

$$H = \begin{pmatrix} 0.8348 & 9.6619 & 2.6591 \\ 0.1002 & 0.0694 & 0.1005 \\ -0.3254 & -8.5837 & -0.9042 \end{pmatrix}. \quad (18)$$

But the network does not synchronize. The states of node 1 are shown in Fig. 21a. Then, let $b = (0, 0, 1)^{\mathrm{T}}$ and $k = (0.0708, -0.15590, 0.4296)$, and then set $H = bk$, so synchronization is achieved as guaranteed by the theory. Figure 21b shows that the states of node 1 quickly reach the equilibrium.

Future Research Outlook

Complex network synchronization is a rapidly growing subject attracting increasing attention from various fields of physics, engineering, mathematics, and biology alike. Despite the current great advances and progress, there are still many important open questions.

In the studies of static coupling, Nishikawa and Motter [48] once pointed out that optimal global synchro-

nizability, with eigenratio being equal to 1, can be obtained from a directed network structure without loops. Even if adding one loop of length 2 (in a directed network, two opposite edges between node i and node j can be considered as a loop of length 2), the eigenratio will be doubled [73,85]. Another scenario is shown by extending the conclusion in [48] to the case of non-identical oscillators [106]. Some further works in this direction will be helpful for in-depth understanding about the role of loops in network synchronization.

In the studies of dynamic coupling, the cost of coupling has not been taken into account. However, cost is usually very significant in some self-driven systems (for example, in wireless sensor networks [107,108] and in distributed autonomous robotic systems [109]). For each node to report its current state to the neighbors (or to detect the states of all its neighbors) requires a certain amount of power, while the total power assigned to each node is often limited, even if such communications are possible. Yet, as found in collective behaviors of biological swarms, a few effective leaders can well organize the whole population [110]. And a recent study has pointed out that partial coupling is more than enough to keep the coherence of self-propelled particles [111]. Therefore, it is very natural to expect to synchronize a complex network with a very low cost, which is an important issue for further investigation.

Very recently, there are some attempts at detecting the network structures with the help of the synchronization phenomenon on complex networks [112,113,114]: to discover the hierarchical community structure by the dynamic time scales of the network synchronization process [112,113], or to infer the complete connectivity of a network from its stable response dynamics [114], etc. These seem quite useful for optimal network design, analy-
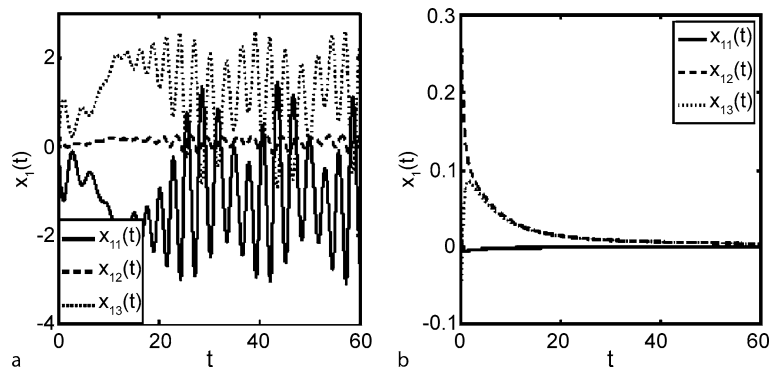
Synchronization Phenomena on Networks, Figure 21
States of node 1 (after [101])

sis, and utilization in general, therefore should be pursued with special efforts.

Similar to the aforementioned open questions, many theoretically attractive and practically important problems about various aspects of synchronization on complex networks can be posted and described. As the network research further evolves in different fields, many new dynamical phenomena and analytic issues will also emerge. Importance notwithstanding, the subject of "Synchronization Phenomenon of Networks" will continue to prove itself an theoretically interesting and technically challenging subject for scientific research in the years to come.

Acknowledgments

Bibliography

1. Albert R, Barabási AL (2002) Rev Mod Phys 74:47
2. Dorogovtsev SN, Mendes JFF (2002) Adv Phys 51:1079
3. Newman MEJ (2003) SIAM Rev 45:167
4. Boccaletti S, Latora V, Moreno Y, Chaves M, Hwang DU (2006) Phys Rep 424:175
5. da F Costa L, Rodrigues FA, Travieso G, Boas PRV (2007) Adv Phys 56:167
6. Pastor-Satorras R, Vespignani A (2001) Phys Rev Lett 86:3200
7. Zhu CP, Xiong SJ, Tian YJ, Li N, Jiang KS (2004) Phys Rev Lett 92:218702
8. Zhou T, Yan G, Wang BH (2005) Phys Rev E 71:046141
9. Zhou T, Fu ZQ, Wang BH (2006) Prog Nat Sci 16:452
10. Zhou T, Liu JG, Bai WJ, Chen GR, Wang BH (2006) Phys Rev E 74:056109
11. Motter AE, Lai YC (2002) Phys Rev E 66:065102
12. Goh KI, Lee DS, Kahng B, Kim D (2003) Phys Rev Lett 91:148701
13. Motter AE (2004) Phys Rev Lett 93:098701
14. Zhou T, Wang BH (2005) Chin Phys Lett 22:1072
15. Galstyan A, Cohen P (2007) Phys Rev E 75:036109
16. Guimerá R, Díaz-Guilera A, Vega-Redondo F, Cabrales A, Arenas A (2002) Phys Rev Lett 89:248701
17. Tadić B, Thurner S, Rodgers GJ (2004) Phys Rev E 69:036102
18. Zhao L, Lai YC, Park K, Ye N (2005) Phys Rev E 71:026125
19. Yan G, Zhou T, Hu B, Fu ZQ, Wang BH (2006) Phys Rev E 73:046108
20. Wang BH, Zhou T (2007) J Korean Phys Soc 50:134
21. Watts DJ, Strogatz SH (1998) Nature 393:440
22. Barabási AL, Albert R (1999) Science 286:509
23. Strogatz SH, Stewart I (1993) Sci Am 269:102
24. Gray CM (1994) J Comput Neurosci 1:11
25. Néda Z, Ravasz E, Vicsek T, Barabási AL (2000) Phys Rev E 61:6987
26. Glass L (2001) Nature 410:277
27. Chen G, Dong X (1998) From Chaos Order. World Scientific, Singapore
28. Erdös P, Rényi A (1960) Pub Math Ins Hung Acad Sci 5:17
29. Wang XF (2002) Int J Bifurc Chaos 12:885
30. Heidelberger R (2007) Nature 450:625
31. Heagy JF, Carroll TL, Pecora LM (1994) Phys Rev E 50:1874
32. Stefański A, Perlikowski P, Kapitaniak T (2007) Phys Rev E 75:016210
33. Wu CW, Chua LO (1995) IEEE Trans Circuits Syst I 42:430
34. Jost J, Joy MP (2001) Phys Rev E 65:016201
35. Gade PM (1996) Phys Rev E 54:64
36. Manrubia SC, Mikhailov AS (1999) Phys Rev E 60:1579
37. Gade PM, Hu CK (1999) Phys Rev E 60:4966
38. Gade PM, Hu CK (2000) Phys Rev E 62:6409
39. Lago-Fernández LF, Huerta R, Corbacho F, Sigüenza JA (2000) Phys Rev Lett 84:2758
40. Wang XF, Chen G (2002) Int J Bifurc Chaos Appl Sci Eng 12:187
41. Wang XF, Chen G (2002) IEEE Trans Circuits Syst I 49:54
42. Barahona M, Pecora LM (2002) Phys Rev Lett 89:054101
43. Jiang PQ, Wang BH, Bu SL, Xia QH, Luo XS (2004) Int J Mod Phys B 18:2674
44. Lind PG, Gallas JAC, Herrmann HJ (2004) Phys Rev E 70:056207
45. Pecora LM, Carrol TL (1998) Phys Rev Lett 80:2109
46. Hu G, Yang J, Liu W (1998) Phys Rev E 58:4440
47. Pecora LM, Barahona M (2005) Chaos Complex Lett 1:61
48. Nishikawa T, Motter AE (2006) Phys Rev E 73:065106
49. Kuramoto Y (1975) In: Araki H (ed) Internaltional Symposium on Mathematical Problems in Theoretical Physics. Lecture Notes in Physics, vol 30. Springer, New York
50. Kuramoto Y (1984) Chemical Oscillations, Wave and Turbulence. Springer, Berlin
51. Kuramoto Y, Nishikawa I (1987) J Stat Phys 49:569
52. Pikovsky A (2001) Synchronization. Cambridge University Press, Cambridge
53. Acebrón JA, Bonilla LL, Vicente CJP, Ritort F, Spigler R (2005) Rev Mod Phys 77:137
54. Nishikawa T, Motter AE, Lai YC, Hoppensteadt FC (2003) Phys Rev Lett 91:014101
55. Newman MEJ, Strogatz SH, Watts DJ (2001) Phys Rev E 64:026118
56. Dorogovtsev SN, Mendes JFF (2000) Phys Rev E 62:1842
57. Hong H, Kim BJ, Choi MY, Park H (2004) Phys Rev E 69:067105
58. Freeman L (1979) Soc Netw 1:215
59. Newman MEJ (2001) Phys Rev E 64:016132
60. Zhou T, Liu JG, Wang BH (2006) Chin Phys Lett 23:2327
61. Fan ZP (2006) Complex Networks: From Topology to Dynamics. Ph D Thesis, City University of Hong Kong
62. Zhao M, Zhou T, Wang BH, Yan G, Yang HJ, Bai WJ (2006) Physica A 371:773
63. Maslv S, Sneppen K (2002) Science 296:910
64. Kim BJ (2004) Phys Rev E 69:045101(R)
65. McGraw PN, Menzinger M (2005) Phys Rev E 72:015101
66. Gómez-Gardeñes J, Moreno Y, Arenas A (2007) Phys Rev Lett 98:034101

67. Wu X, Wang BH, Zhou T, Wang WX, Zhao M, Yang HJ (2006) Chin Phys Lett 23:1046
68. Holme P, Kim BJ (2002) Phys Rev E 65: 026107
69. Newman MEJ (2002) Phys Rev Lett 89:208701
70. di Bernardo M, Garofalo F, Sorrentino F (2007) Int J Bifurc Chaos 17:3499
71. Sorrentino F, di Bernardo M, Cuéllar GH, Boccaletti S (2006) Physica D 224:123
72. Chavez M, Hwang DU, Martinerie J, Boccaletti S (2006) Phys Rev E 74:066107
73. Zhao M, Zhou T, Wang BH, Ou Q, Ren J (2006) Eru Phys J B 53:375
74. Huang L, Park K, Lai YC, Yang L, Yang K (2006) Phys Rev Lett 97:164101
75. Radicchi F, Castellano C, Cecconi F, Loreto V, Parisi D (2004) Proc Natl Acad Sci USA 101:2658
76. Zhou T, Zhao M, Chen G, Yan G, Wang BH (2007) Phys Lett A 368:431
77. Donetti L, Hurtado PI, Muñoz MA (2005) Phys Rev Lett 95:188701
78. Motter AE, Zhou C, Kurths J (2005) Phys Rev E 71:016116
79. Motter AE, Zhou C, Kurths J (2005) Europhys Lett 69:334
80. Motter AE, Zhou C, Kurths J (2005) AIP Conf Proc 776:201
81. Hwang DU, Chavez M, Amann A, Boccaletti S (2005) Phys Rev Lett 94:138701
82. Dorogovtsev SN, Mendes JFF, Samukhin AN (2000) Phys Rev Lett 85:4633
83. Krapivsky PL, Redner S (2001) Phys Rev E 63:066123
84. Zou Y, Zhu J, Chen G (2006) Phys Rev E 74:046107
85. Chavez M, Hwang DU, Amann A, Hentschel HGE, Boccaletti S (2005) Phys Rev Lett 94:218701
86. Chavez M, Hwang DU, Amann A, Boccaletti S (2006) Chaos 16:015106
87. Goh KI, Kahng B, Kim D (2001) Phys Rev Lett 87:278701
88. Wang X, Lai YC, Lai CH (2007) Phys Rev E 75:056205
89. Zhou C, Kurths J (2006) Phys Rev Lett 96:164102
90. Huang D (2006) Phys Rev E 74:046208
91. Boccaletti S, Hwang DU, Chavez M, Amann A, Kurths J, Pecora LM (2006) Phys Rev E 74:016102
92. Zhao M, Zhou T, Wang BH, Wang WX (2005) Phys Rev E 72:057102
93. Barthélemy M (2004) Eur Phys J B 38:163
94. Zhou T, Zhao M, Wang BH (2006) Phys Rev E 73:037101
95. Bondy JA, Murty USR (1976) Graph Theory with Applications. MacMillan, London
96. Bollobás B (1998) Modern Graph Theory. Springer, New York
97. Xu JM (2003) Theory and Application of Graphs. Kluwer, Dordrecht
98. Newman MEJ, Watts DJ (1999) Phys Rev E 60:7332
99. Yin CY, Wang WX, Chen G, Wang BH (2006) Phys Rev E 74:047102
100. Comellas F, Gago S (2007) J Phys A Math Theor 40:4483
101. Duan Z, Chen G, Huang L (2007) Phys Rev E 76:056103
102. Duan Z, Chen G, Huang L (2007) Phys Lett A 372:3741
103. Duan Z, Liu C, Chen G (2008) Physica D 237:1006
104. Friedland B (1986) Control System Design. McGraw-Hill, New York
105. Tsuneda A (2005) Int J Bifurc Chaos 15:1
106. Um J, Han SG, Kim BJ, Lee SI (2008) (unpublished)
107. Akyildiz IF, Su W, Sankarasubramaniam Y, Cayirci E (2002) Comput Netw 38:393
108. Oqren P, Fiorelli E, Leonard NE (2004) IEEE Trans Automat Contr 49:1292
109. Arai T, Pagello E, Parker LE (2002) IEEE Trans Robot Automat 18:655
110. Couzin LD, Krause J, Franks NR, Levin SA (2005) Nature 433:513
111. Zhang HT, Chen M, Zhou T (2007) arXiv:0707.3402
112. Arenas A, Díaz-Guilera A, Pérez-Vicente CJ (2006) Phys Rev Lett 96:114102
113. Boccaletti S, Ivanchenko M, Latora V, Pluchino A, Rapisarda A (2007) Phys Rev E 75:045102(R)
114. Timme M (2007) Phys Rev Lett 98:224101

Synergetics: Basic Concepts

HERMANN HAKEN
Institut für Theoretische Physik, Universität Stuttgart, Stuttgart, Germany

Article Outline

Glossary

Synergetics Science of cooperation.

Pattern A pattern is essentially an arrangement. It is characterized by the order of the elements of which it is made rather than by the intrinsic nature of these elements (Norbert Wiener).

Self-organization Formation of spatio-temporal patterns (structures) and/or performance of functions without an "ordering hand".

State vector Set of time- or time-independent variables that characterize the state of a system.

Evolution equations Determine the temporal evolution of the state vector. May be deterministic, stochastic or both.